Modeling of Tsunami Fluid Force on a Bridge Deck Subjected to Plunging Breaker Bores and Surging Breaker Bores

G. Shoji & Y. Ezura
University of Tsukuba, Japan

Y.Hiraki
Central Japan Railway Company, Japan

SUMMARY:
The 2011 off the Pacific Coast of Tohoku earthquake tsunami caused the catastrophic damage of infrastructures such as coastal structures, utilities and transportation facilities. Among the infrastructures evaluation of tsunami fluid force acting on a bridge deck is urgently required for designing a tsunami-proof bridge structure. Authors carried out hydraulic experiments to clarify the mechanism of tsunami wave loads acting on a bridge deck subjected to plunging breaker bores and surging breaker bores, focusing on the relationship between the position of a bridge deck to a wave height and the occurrence of horizontal and vertical wave forces acting on a bridge deck.

Keywords: Tsunami fluid force, bridge deck, plunging breaker bore, surging breaker bore

1. INTRODUCTION

The 2011 off the Pacific Coast of Tohoku earthquake tsunami caused the catastrophic damage of infrastructures such as coastal structures, utilities and transportation facilities. Among them a bridge structure plays important roles to carry out emergency response by related stakeholders and to support their recovery activities. Thus, since the 2004 Indian Ocean tsunami disaster, evaluation of tsunami fluid forces acting on a bridge deck is urgently required for designing a tsunami-proof bridge structure, and many academic researchers and practitioners are involved in this issue.

The related experimental research from Kataoka *et al.*(2006) validated the formulas by Goda (1973) for calculating horizontal wave force acting on a bridge deck. Shoji and Mori (2006) validated the formulas by Matsutomi and Iizuka (1998) for adopting the computation of tsunami current velocity in front of a bridge deck and in the rear of it. In addition, Araki *et al*. (2008) revealed the mechanism of vertical wave force on a bridge deck and clarified the relation between horizontal wave force and the position of a bridge deck to a wave height. Shoji *et al*. (2009) evaluated the dependency of a bridge deck movement on tsunami wave forces by hydraulic experiments considering similarity laws. Nii *et al*. (2009) compared the experimental results with the existing design formulation by Goda (1973) on the evaluation of horizontal pressure on a breakwater subjected to a tsunami, and Nakao *et al*. (2009) showed the flow vortex induced on a bridge deck by a tsunami wave from hydraulic experiments.

However, the effect of types of breaker bores on the evaluation of a drag coefficient and a lift coefficient is not revealed, and the dependency of changes of the position of a bridge deck to a tsunami wave height on the variation of horizontal and vertical wave forces has not been clarified enough. Based on the above, we evaluate the tsunami wave forces on a single spanned RC bridge deck subjected to plunging breaker bores and surging breaker bores by hydraulic experiments.

2. HYDRAULIC EXPERIMENTS

Table 2.1 shows experimental cases and Fig. 2.1 shows the experimental setups. Plunging breaker bores are idealized as those acting on a bridge deck near river mouth. In the case, a bridge deck model is set up at 1,500mm from Point-0. Surging breaker bores are idealized as those acting on a bridge deck in the river run-up zone. In the case, a bridge deck model is set up at 5,500mm from Point-0.

Table 2.1. Test cases (*BB: Breaker bores, SBB: Surging breaker bores, PBB: Plunging breaker bores, SWL: Still water level)

CASE No.		Types of BB*	SWL* h_0 (mm)	Height from lower level of a deck to SWL h_c (mm)	Tank water level (mm)	CASE No.		Types of BB*	SWL* h_0 (mm)	Height from lower level of a deck to SWL h_c (mm)	Tank water level (mm)
	1				430		1				410
1	2	SBB	50	0	440	9	2	PBB	50	0	420
	3				450		3				430
	1				430		1				402
2	2	SBB	45	5	440	10	2	PBB	45	5	412
	3				450		3				420
	1				425		1				410
3	2	SBB	40	10	435	11	2	PBB	40	10	420
	3				445		3				430
	1				425		1				390
4	2	SBB	35	15	435	12	2	PBB	35	15	400
	3				445		3				410
	1				425		1				390
5	2	SBB	30	20	435	13	2	PBB	30	20	400
	3				445		3				410
	1				425		1				410
6	2	SBB	25	25	435	14	2	PBB	25	25	415
	3				445		3				420
	1				425		1				420
7	2	SBB	20	30	435	15	2	PBB	20	30	425
	3				445		3				430
	1				460		1				440
8	2	SBB	10	40	465	16	2	PBB	10	40	445
	3				470		3				450

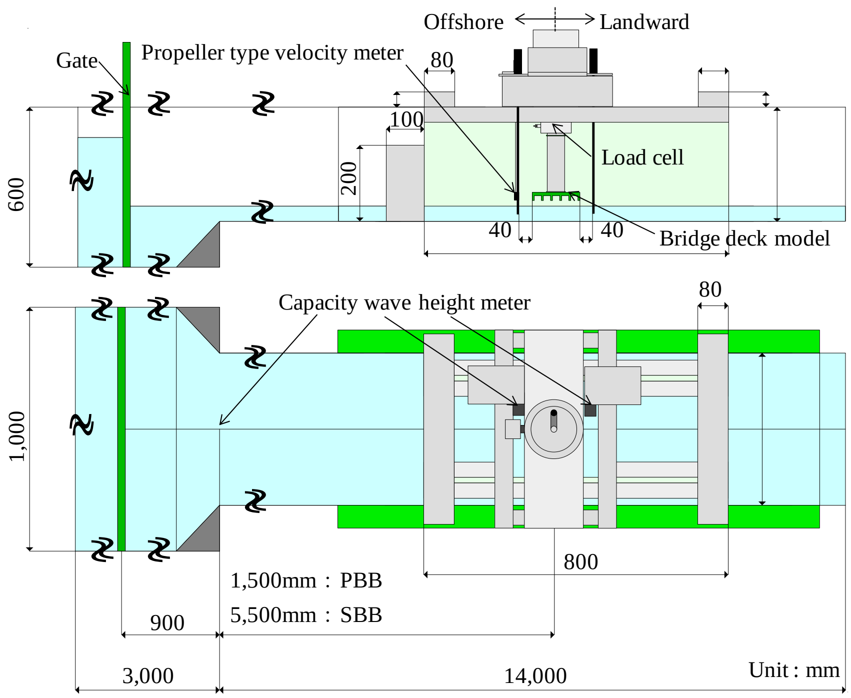

Figure 2.1. Experimental setups

Figure 2.2 shows the length, height and width of a bridge deck model. The model is geometrically

1/79.2 scaled down from a prototype bridge: the Lueng Ie Bridge at Sumatra Island which was affected by the Indian Ocean tsunami. We vary the still water level h_0 from 50mm to 20mm at a 5mm interval, and h_0 from 20mm to 10mm at a 10mm interval. For each case, we generate breaker bores with still water level h_0 by opening the gate of the water flume manually after gradually increasing the water height. We measure tsunami velocity in front of a bridge deck by propeller type velocity meter (KENEK Co., VOT2-100-10), wave heights at the Point-0 and at the 40 mm in front of a deck by the capacity wave height meters (MASATOYO ENG Co., L-300) and horizontal wave force, vertical wave force, and moment on a bridge deck by load cell (NIKKEI ELECTRONIC INSTRUMENTS CO. LTD., Y102). They are recorded at a sampling rate of 200 Hz for 20 seconds from the gate opening. We average the values of data by moving averaged method by using each 10 data before and after subject recorded point. In all cases we carried out experiments with a bridge deck and without a bridge deck, and we repeated experiments to obtain 3 reliable data for each case. In the following analysis we use the data of horizontal wave force and vertical wave force with a bridge deck, and the data of tsunami velocity and tsunami wave height without a bridge deck. We cannot gain the reliable velocity data for CASE1-1, 3-1, 6-1, 9-1, 13-1, 15-1, 15-2 in Table 2.1. Figure 2.3 shows the important parameters on a tsunami wave load for analysis.

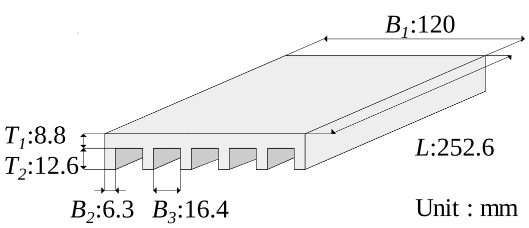

Figure 2.2. Bridge deck model

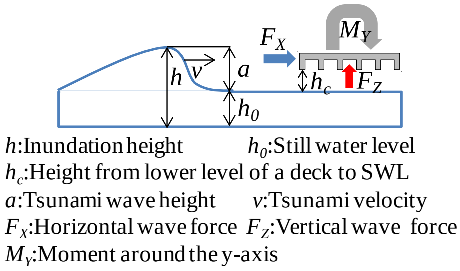

Figure 2.3. Parameters on a tsunami wave load

3. EVALUATION OF DRAG COEFFICIENT AND LIFT COEFFICIENT

For analysis we use the horizontal wave force F_X, tsunami velocity v, and tsunami wave height a which are measured at the impulsive moment when a tsunami wave reaches to a bridge deck. The average values of F_X and a for repeating times of each experimental case number are computed as $\overline{F_X}$ and $\overline{a}$, and average value of square of v is also computed as $\overline{v^2}$. The value of drag coefficient C_D is computed as follows,

$$C_D = \frac{\overline{F_X}}{\frac{1}{2}\rho \overline{v^2} A_s} \tag{3.1}$$

where ρ is the density mass of unit volume of water, and A_s is the projected area of a bridge deck subjected to a tsunami wave in the horizontal direction.

In addition, the values of wave velocity v and wave height a for 1 to 3 seconds after their peaks of wave velocity and wave height are averaged to be defined as averaged tsunami velocity v_{ave} and averaged wave height a_{ave}. The averaged values of v_{ave} and a_{ave} for the experimental repeating times are computed as $\overline{v_{ave}}$ and $\overline{a_{ave}}$. And averaged inundation height $\overline{h_{ave}}$ is computed by adding h_0 to $\overline{a_{ave}}$.

The value of Froude number F_r is computed as follows,

$$F_r = \frac{\overline{v_{ave}}}{\sqrt{g\overline{h_{ave}}}} \tag{3.2}$$

where g is gravity acceleration.

Figure 3.1 shows the relation between drag coefficient C_D and Froude number F_r. From Fig. 3.1, for surging breaker bores C_D shows the range from 1.43 to 2.36, whereas F_r shows the range from 0.41 to 0.60. For plunging breaker bores C_D shows the range from 1.19 to 2.21, whereas F_r shows the range from 0.43 to 0.78. The maximum value of C_D for surging breaker bores is 1.07 times larger than that for plunging breaker bores.

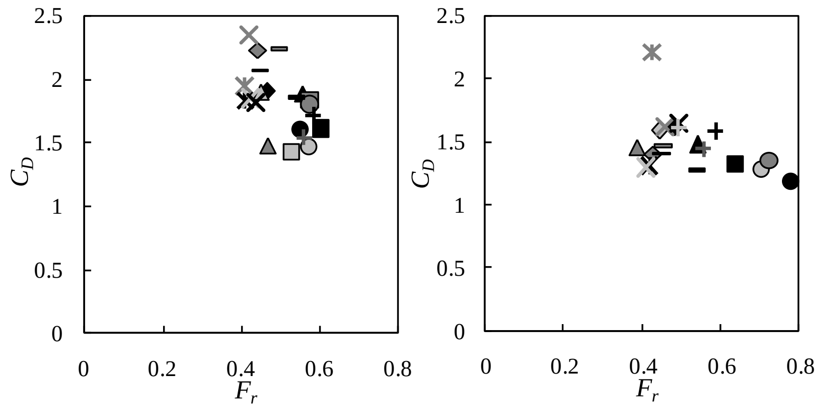

(a) For surging breaker bores **(b)** For plunging breaker bores

Figure 3.1. Relation between C_D and F_r

CASE1-1,9-1 (SWL50mm)	CASE1-2,9-2 (SWL50mm)	CASE1-3,9-3 (SWL50mm)
CASE2-1,10-1 (SWL45mm)	CASE2-2,10-2 (SWL45mm)	CASE2-3,10-3 (SWL45mm)
CASE3-1,11-1 (SWL40mm)	CASE3-2,11-2 (SWL40mm)	CASE3-3,11-3 (SWL40mm)
CASE4-1,12-1 (SWL35mm)	CASE4-2,12-2 (SWL35mm)	CASE4-3,12-3 (SWL35mm)
CASE5-1,13-1 (SWL30mm)	CASE5-2,13-2 (SWL30mm)	CASE5-3,13-3 (SWL30mm)
CASE6-1,14-1 (SWL25mm)	CASE6-2,14-2 (SWL25mm)	CASE6-3,14-3 (SWL25mm)
CASE7-1,15-1 (SWL20mm)	CASE7-2,15-2 (SWL20mm)	CASE7-3,15-3 (SWL20mm)
CASE8-1,16-1 (SWL10mm)	CASE8-2,16-2 (SWL10mm)	CASE8-3,16-3 (SWL10mm)
CASE1 to 8 represent SBB	CASE9 to 16 represent PBB	

We use vertical wave force F_Z which is measured at the impulsive moment when a tsunami wave reaches to a bridge deck. The average value of F_Z for the experimental repeating times is computed as $\overline{F_Z}$. The value of lift coefficient C_L is computed as follows,

$$C_L = \frac{\overline{F_Z}}{\frac{1}{2}\rho \overline{v^2} A_b} \tag{3.3}$$

where A_b is the projected area of a deck subjected to vertical wave force: the area of a bottom of a bridge deck.

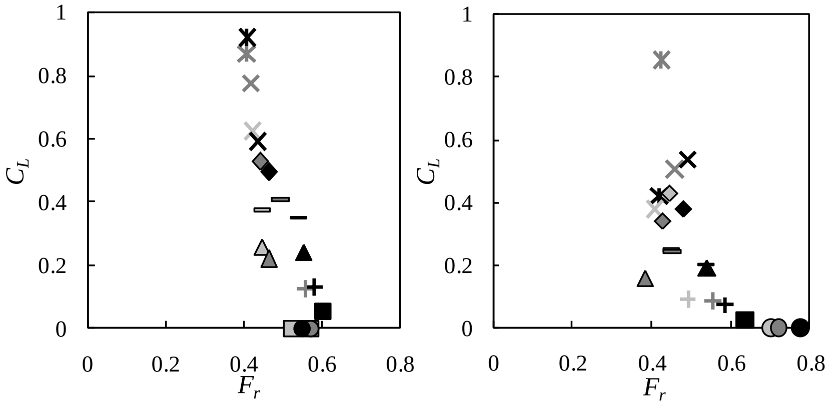

(a) For surging breaker bores **(b)** For plunging breaker bores

Figure 3.2. Relation between C_L and F_r (Same legends at Fig.3.1)

Figure 3.2 shows the relation between lift coefficient C_L and Froude number F_r. The values of F_Z in the cases that uplift vertical wave force didn't occur show zero: in the cases C_L shows zero. From Fig. 3.2, for surging breaker bores C_L shows the range from 0.05 to 0.92, whereas F_r shows the range from 0.41 to 0.60. For plunging breaker bores C_L shows the range from 0.02 to 0.86, whereas F_r shows the range from 0.43 to 0.64. By referring the results by Oba and Bando (2006), the value of C_L varies from -0.4 to 1.6 when the angle of attack α to a bridge deck in the horizontal direction changes from -8 degrees to 16 degrees. In terms of the maximum value of C_L, the meanings of C_L = 0.92 for surging breaker bores and of C_L = 0.86 for plunging breaker bores are that the tsunami wave crest acts on a bridge deck with angle of attack α of 5.2 degrees for surging breaker bores and with angle of attack α of 4.6 degrees for plunging breaker bores.

4. EVALUATION OF HORIZONTAL AND VERTICAL PRESSURE ON A BRIDGE DECK

Non-dimensional parameter κ is defined as the following Eqn. 4.1, which means the magnification factor of horizontal wave pressure compared with hydrostatic pressure on a bridge deck corresponding to wave height $\bar{a}$.

$$\kappa = \frac{\overline{F_X} / A_s}{\rho g \bar{a}} \tag{4.1}$$

Parameter η is defined as the value of the height from lower level of a bridge deck to the crest of a wave ($\bar{a}$-h_c) divided by wave height $\bar{a}$.

Figure 4.1 shows the relation between κ and η. For surging breaker bores, κ varies from 1.10 to 1.79 when η varies from 0.24 to 0.71. In the range of η, the horizontal wave pressure on a bridge deck is larger than that in the other range of η from 0.79 to 1.00. κ is decreasing from 1.55 to 0.89 when η increases from 0.79 to 1.00. In the range of η, κ becomes weaker than one in the other range of η from 0.24 to 0.71. For plunging breaker bores, κ varies from 1.35 to 2.02 when η varies from 0.21 to 0.65. In the range of η, the horizontal wave pressure on a bridge deck is larger than that in the other range of η from 0.75 to 1.00. κ is decreasing from 1.71 to 1.03 when η increases from 0.75 to 1.00. In the range of η, κ becomes weaker than one in the other range of η from 0.21 to 0.65. The trend of dependency of κ on η for surging breaker bores is almost same as that for plunging breaker bores, however the values of κ for plunging breaker bores are larger than those for surging breaker bores.

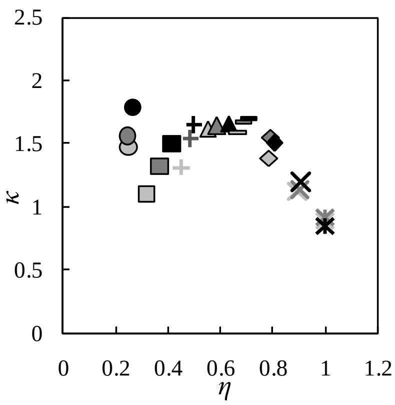

(a) For surging breaker bores

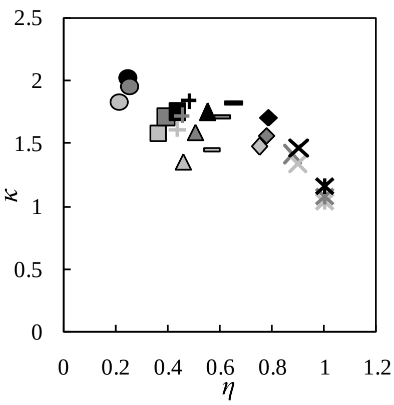

(b) For plunging breaker bores

Figure 4.1. Relation between κ and η (Same legends at Fig.3.1)

In the similar way, non-dimensional parameter λ is defined as the following Eqn. 4.2, which shows the magnification factor of vertical wave pressure compared with hydrostatic pressure on a bridge deck corresponding to wave height $\bar{a}$.

$$\lambda = \frac{\overline{F_Z}/A_b}{\rho g \bar{\bar{a}}} \tag{4.2}$$

Figure 4.2 shows the relation between λ and η. For surging breaker bores, the vertical wave pressure shows zero in the range of η from 0.27 to 0.37, which means vertical wave pressure does not occur on a bridge deck. In the range of η over 0.41, vertically positive wave pressure of λ=0.05 occurs on a bridge deck. λ varies from 0.05 to 0.41 when η varies from 0.41 to 1.00. For plunging breaker bores, the vertical wave pressure shows zero in the range of η from 0.21 to 0.25, which means vertical wave pressure does not occur on a bridge deck. In the range of η over 0.39, vertically positive wave pressure of λ=0.04 occurs on a bridge deck. λ varies from 0.04 to 0.48 when η varies from 0.39 to 1.00. Uplift vertical wave pressure becomes large when the position of a bridge deck to a wave height becomes low, which is opposite trend to the decrease of horizontal wave pressure for η. The trend of dependence of λ on η for surging breaker bores is almost same as that for plunging breaker bores, however the values of λ for plunging breaker bores are larger than those for surging breaker bores.

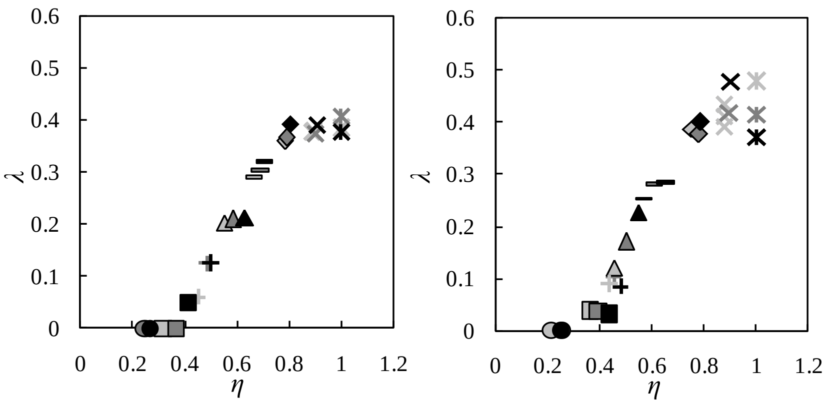

(a) For surging breaker bores **(b)** For plunging breaker bores

Figure 4.2. Relation between λ and η (Same legends at Fig. 3.1)

For both breaker bores, horizontal wave pressure is high with smaller uplift vertical wave pressure in the case that the position of a bridge deck to a wave height is high, whereas both horizontal wave pressure and vertical wave pressure act on a bridge deck in the case that the position of a bridge deck to a wave height is low, as shown in Fig. 4.3. Furthermore, horizontal wave pressure and vertical wave pressure for plunging breaker bores is larger than those for surging breaker bores. Hence, from the viewpoint of a tsunami wave load on a bridge deck, plunging breaker bores are more severe loads than surging breaker bores.

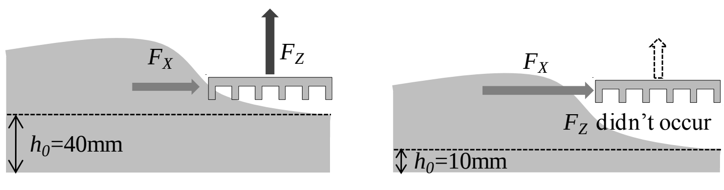

(a) SWL=40mm **(b)** SWL=10mm

Figure 4.3. The mechanism of a tsunami wave load subjected to a bridge deck

5. CONCLUSIONS

Authors carried out hydraulic experiments to clarify a tsunami wave load on a bridge deck subjected to plunging breaker bores and surging breaker bores, focusing on the relationship between the position of a bridge deck to a wave height and the occurrence of horizontal and vertical wave forces acting on a bridge deck. Following results are reduced.

For surging breaker bores C_D shows the range from 1.43 to 2.36, whereas F_r shows the range from 0.41 to 0.60. For plunging breaker bores C_D shows the range from 1.19 to 2.21, whereas F_r shows the range from 0.43 to 0.78. The maximum value of C_D for surging breaker bores is 1.07 times larger than that for plunging breaker bores.

For surging breaker bores C_L shows the range from 0.05 to 0.92, whereas F_r shows the range from 0.41 to 0.60. For plunging breaker bores C_L shows the range from 0.02 to 0.86, whereas F_r shows the range from 0.43 to 0.64. In terms of the maximum value of C_L, the meanings of C_L = 0.92 for surging breaker bores and of C_L = 0.86 for plunging breaker bores are that the tsunami wave crest acts on a bridge deck with angle of attack α of 5.2 degrees for surging breaker bores and with angle of attack α of 4.6 degrees for plunging breaker bores.

For both breaker bores, horizontal wave pressure is high with smaller uplift vertical wave pressure in the case that the position of a bridge deck to a wave height is high, whereas both horizontal wave pressure and vertical wave pressure act on a bridge deck in the case that the position of a bridge deck to a wave height is low. Horizontal wave pressure and vertical wave pressure for plunging breaker bores are larger than those for surging breaker bores.

AKCNOWLEDGEMENT

We appreciate the generous supports for using hydraulic experimental facility at Department of Civil and Environmental Engineering, National Defense Academy of Japan from Professor K. Fujima and Professor Y. Shigihara. We also appreciate the valuable supports for the preparation and operation of series of hydraulic experiments, provided by Mr. M. Iidaka at University of Tsukuba.

REFERENCES

Araki, S., Nakajima, H., Deguchi, I. and Itoh, S. (2008). Experimental study on tsunami fluid force acting on bridge beam near river mouth. *Proceedings of Coastal Engineering*, Japan Society of Civil Engineers. **55**, 866-870.

Goda, Y. (1973). A new method of wave pressure calculation for the design of composite breakwaters. *Report of the Port and Harbour Research Institute*. **2:3**, 35-68.

Kataoka, S., Kusakabe, T. and Nagaya, K. (2006). Wave force acts on a bridge girder struck by tsunami. *Proceedings of the 12th Japan Earthquake Engineering Symposium*. 154-157.

Matsutomi, H. and Iizuka, H. (1998). Tsunami current velocity on land and its simple estimation method. *Proceedings of Coastal Engineering*, Japan Society of Civil Engineers. **45**, 361-365.

Nakao, H., Izuno, K. and Kobayashi, H. (2009). Flow and hydrodynamic force characteristics associated with a tsunami acting on a bridge. *Journal of Structure Engineering*, Japan Society of Civil Engineers. **55:A**, 789-798.

Nii, S., Kosa, K., Shoji, G. and Kimura, K. (2009). Experimental examination concerning tidal wave action power to bridge. *Journal of Structure Engineering*, Japan Society of Civil Engineers. **55:A**, 471-482.

Oba, K. and Bando, K. (2006). Fluid Mechanics, Corona Publishing Co., Ltd., Japan.

Shoji, G. and Mori, Y. (2006). Experimental study on tsunami damage of a bridge deck. *Journal of Coastal Engineering*, Japan Society of Civil Engineers. **53**, 801-805.

Shoji, G., Moriyama, T., Hiraki,Y., Fujima,K., Shigihara,Y. and Kasahara, K. (2009). Evaluation of a tsunami wave load acting on a bridge deck subjected to plunging breaker bores and surging breaker bores. *Journal of Coastal Engineering*, Japan Society of Civil Engineers. **56:2**, 826-830.